



Total Control

*Advanced integrated supervisory and wind turbine control
for optimal operation of large Wind Power Plants*

Probabilistic framework to quantify the reliability
levels of wind turbine structures under enhanced
control methods
Deliverable D2.5

Delivery date: 20.01.2020
Lead beneficiary: DTU
Dissemination level: Public



This project has received funding
from the European Union's Horizon
2020 Research and Innovation
Programme under grant agreement
No. 727680

Author(s) information (alphabetical):		
Name	Organisation	Email
Nikolay Dimitrov	DTU	nkdi@dtu.dk
Anand Natarajan	DTU	anat@dtu.dk

Acknowledgements/Contributions:		
Name	Name	Name
Shadan Mozafari	DTU	shmoz@dtu.dk

Document information

Version	Date	Description	Prepared by	Reviewed by	Approved by
1	15.01.2020	Authors		Malene Pogager	Gunner Chr. Larsen

Definitions/Abbreviations

AEP	Annual energy production
ANN	Artificial neural network
CAPEX	Capital expenditures
CDF	Cumulative distribution function
LCOE	Levelized cost of energy

TABLE OF CONTENTS

Executive summary	4
1. Introduction.....	5
1.1. State of the Art in load modeling	6
1.2. Wind Farm Model dependencies.....	7
2. Probabilistic models for wind farm control.....	10
2.1. Probabilistic models	10
2.1.1 Ultimate Limit State Analysis.....	10
2.1.2 Fatigue Limit State Analysis.....	11
2.2. Design Limits.....	12
2.3. Remaining Life Estimation.....	14
2.4. Baseline Case at Lillgrund	14
3. Load Alleviation using surrogate models.....	16
3.1. Fitting procedure and validation of load and power predictions at Lillgrund.....	16
4. Wind Farm Performance for target reliability	21
4.1. Predicted annual reliability under operating conditions	21
4.2. Performance optimization.....	24
5. Wind farm cost Impact.....	26
6. Conclusions	28
References	29

EXECUTIVE SUMMARY

Probabilistic methods for assessing the fatigue life consumption of wind turbines in the Lillgrund wind farm are implemented, so that the impact of selective curtailment of leading wind turbines in the farm on the production and remaining life are determined. The probabilistic models for fatigue failure are established using the fatigue life cycle curve (SN) approach together with the Miner rule of linear fatigue damage accumulation. Standard SN-curves are used to model the fatigue damage and uncertainty related to the loads models and material are incorporated. The probabilistic methods are based on assessing the annual reliability level of wind turbine structures using damage equivalent loads as a function of the position in the farm and comparing with the required annual reliability level used in the design process.

To enable this assessment, loads simulations are made over the full wind farm with varying mean wind speeds and wind directions. The effects of wakes in the wind farm are quantified using the dynamic wake meandering model. Conditions whereby the leading row wind turbines are curtailed by different percentages are also simulated. The results from the load simulations are used to train a surrogate model, i.e. an artificial neural network (ANN) to be able to represent the damage equivalent loads at the blade root, main shaft and tower base, given the free stream wind conditions. The ANN is then used to simulate several wind directions and wind speeds across the wind farms to quickly compute the power production and damage consumption with and without de-rating. Validations of the simulations are made with measured loads on one of the wind turbines and with power production measurements over all wind turbines. De-rating the wind turbines in the second row of the wind farm by about 20% was determined to produce the best benefit in increase in annual energy production (AEP) and load reduction. At 9m/s mean wind speed, the benefit was maximum with about 20% load reduction on the highest loaded wind turbines and 40% increase in power production in the worst producing turbines. There is a significant net power gain for the full wind farm when applying the above de-rating strategy at wind speeds between 5m/s and 13m/s, and for wind directions of about plus-minus 12 degrees from the wind turbine row alignments. The overall lifetime AEP gain without life extension is approximately 2%, when considering the joint wind speed and wind direction distributions at Lillgrund.

The reduction in load also implies that the wind farm lifetime can be extended. Since the slope of the SN curve is non-linear, even a small increase in load level can result in a large increase in fatigue life. It is estimated that a short duration of de-rating of 20% with the second row can increase the life of the wind farm by about 5 years. When combined with the increase in AEP, this can result in an LCOE reduction of at least 3% for the Lillgrund wind farm.

1. INTRODUCTION

In large offshore wind farms, the mechanical loading and power production of individual turbines can vary significantly depending on the turbine location in the park, due to the effect of wakes or variations in the free-wind conditions. Nevertheless, the turbines in a wind farm typically have similar rotor-nacelle assemblies designed to withstand wind conditions corresponding to a reference type class [1], and consideration of the site-specific conditions is only given to the support structure design and to ensure that the loads on the worst-affected turbine in the farm do not exceed the design limit. Therefore the fatigue loads accumulated by turbine structures within the farm can vary significantly. Mapping the variation of fatigue load exposure on farm level is relevant for a number of engineering purposes such as prediction of life consumption, estimating the remaining lifetime, enabling inspections, maintenance and service, so as to focus on the highest loaded turbines.

Optimization of the energy production in the windfarms is also very important. In other words, there is a strong focus on getting as much energy as possible from the wind turbines within their design limits. The main barrier for increased energy production is the limited distance between wind turbines in the wind farm leading to pronounced wake effects. The wake is the region of turbulent flow downstream of the wind turbine. As the flow proceeds downstream, there is a spreading of the wake and multiple wakes, eventually recovering towards free stream conditions. The wake effect is especially significant in offshore windfarms, where the number of the wind turbines is often very high. There are several studies done on deriving wind farm and wind turbine controller schemes in order to mitigate the loads on the components of the WT [2], [3], [4], which also affects the lifetime of the components and their extension. There are some recent work like [5], [6], and [7] on investigating specific supervisory controlling strategies directly based on lifetime and fatigue damage in the WT. However implementing such controlling schemes for wind farms with the intent to control fatigue is typically not done commercially.

Another reason that fatigue consumption for primary structures of a wind turbine need to be evaluated is due to the reason that wind farms must achieve very long operating lives in order to lower the Levelized Cost of Energy (LCOE). Progress in the development of modern wind turbines has been paced by progress in our understanding of fatigue loads, modeling of structural-dynamic responses to unsteady winds, and the design of structural elements to resist these responses [8]. Degradation models are used to model and predict degradation of items. Degradation can be expressed and measured by a quantity which describes in a suitable way the changing of the technical condition or strength over time (or another measure of usage). This quantity is denoted degradation variable. Failure is assumed to occur when the value of a degradation variable crosses a failure level (threshold). In some applications, there may be more than one degradation variables [9]. Cumulative damage theories consider the fatigue process to be one of damage accumulation until the life of the component is exhausted. Palmgren Miner rule [10] is a accumulative linear damage accumulation rule that while being simple and possibly non-physical is extensively used in the design process of wind turbines. It has limitations such as not considering the loading sequencing effects (which may be very important). Due to all the uncertainties and complexities mentioned, full deterministic models without considering the uncertainties are not used for fatigue lifetime estimation. Instead the probability of failure due to different mechanisms (including fatigue) is estimated.

The practices of modeling and failure analysis require an assessment of the site-specific component loads, based on the turbine's operational history and measured wind conditions, along with a probabilistic analysis contingent on the current structural condition and the impact of possible material degradation on the structure's fatigue limit state. The main factors in such models can be classified as damage rules, load spectra, material properties and solution techniques. Furthermore, these models should be capable of considering various material properties. When considering fatigue design evaluation, it is convenient to establish both the material resistance and the component loads as equivalent fatigue loads. The advantage of this concept is that any load time history, can be reduced to one number, which greatly increases computational efficiency. The turbine equivalent fatigue load is the load that, when applied N_{eq} times, would produce the same amount of fatigue damage as the actual random load history; it is found by calculating the load history representative for the turbine's life under the set of site conditions with rainflow counting all load cycles in its history.

A probabilistic model of the turbine structure can be based on wind conditions, loads, and material-degradation models and reflect the inspection report. It would be a valuable tool that accurately estimates the remaining life-time and predicts the schedule for maintenance that can prolong the components' lifetime and prevent future failures [11]. Stochastic, data driven models are based on probability theory and statistical methods. Data-driven models and Artificial Intelligence (AI) based models are based on methods to identify and abstract information and/or relationships from large sets of data [12]. Data-driven methods are in particular suitable for wind farms with continuous monitoring. Many data-driven models belong to the field of AI, which is a rapidly evolving discipline that is beginning to be used in wind farm operational diagnostics.

The Lillgrund Wind Farm is located about 10 km off the coast of southern Sweden, just south of the Öresund Bridge. It has 48 Siemens SWT-2.3-93 wind turbines and a capacity of 110MW. The wind turbines are mounted on gravity based support structures. The remaining sections in this document will focus on applying probabilistic models to load simulation and experimental results obtained from Lillgrund.

1.1. State of the Art in load modeling

The HAWC2 aeroelastic software [13] is used for all load simulations herein and this is a state-of-the-art loads simulation code used by industry and academia. The results from load simulations can be used to fit models that can represent the loads for a certain range of input wind conditions. Functions providing quick, continuously differentiable load predictions with reasonable uncertainty can be obtained by means of surrogate models trained on databases with high-fidelity load simulations. The surrogate models may build on a variety of numerical methods [12], but a widely used method is to train a specific artificial neural network (ANN) to be able to output the wind turbine loads and power production within a wind farm, given a set of inputs that include the free stream wind conditions. The state-of-the-art regarding wake modelling is the dynamic wake meandering model, which is one of the recommended models in the IEC 61400-1 Ed. 4.

Due to the importance of wake effects in reducing energy production and increasing loads, there has been much interest in minimising wake effects through wind farm control, that is the wind farm controller alters the operation of individual turbines in order to achieve the optimum performance of the wind farm as a whole. In this deliverable, the only wind farm control aspect that is utilized is de-rating or curtailment of the wind turbines. Other control aspects such as up-rating, yaw steering [14] etc. exist which may be applicable in different scenarios.

1.2. Wind Farm Model dependencies

The objectives of Deliverable 2.5 requires that a surrogate model is developed which can estimate power and loads for individual turbines in a wind farm, where each turbine could have a different derating level. Since such a model is intended as a part of a gradient-based optimization procedure, it needs to be computationally efficient and be continuously differentiable (e.g. at least the first derivative of the response should exist and should be a continuous function). Experiences from earlier works [12], [15], show that a suitable approach could be the use of surrogate models trained on a large number of aeroelastic load simulations. With the surrogate model approach, a load response database is created by carrying out load simulations under various conditions aiming at covering a predefined input variable space. Then, a regression model is trained which maps the dependence of the load simulation outputs on the input variables. For the present problem, the following variable space is required:

- \mathbf{X}_{amb} : variables representing the ambient, free-wind conditions (wind speed, turbulence, wind direction)
- \mathbf{X}_{op} : variables describing the operating status of the turbines under consideration (in the present case, this is the derating level, from 0 to 95% of nominal power, in 5% steps, where 0% means full nominal power, and 100% derating means no power output). Note that 100% derating is equivalent to the turbine being non-operational.
- \mathbf{X}_{farm} : variables describing the farm effects in terms of the relative positions of turbines. For any given turbine in the wind farm, these variables consist of the distance (in rotor diameters) to an upwind turbine, R_D , and θ , the relative angle between the direction to the upwind turbine and the wind direction (wind-wake misalignment). If the upwind turbine is derated, a third variable is necessary – the derating level, in this case from 0 to 100%, in 5% steps. Note that a 100% derating of upwind turbines is equivalent to the upwind turbine being non-operational. If there are more than one disturbing turbines upwind, one set of \mathbf{X}_{farm} variables is needed for each upwind turbine. For example, if there are 5 disturbing turbines considered, a total of $5 \times 3 = 15$ \mathbf{X}_{farm} variables are necessary.

The approach of defining the \mathbf{X}_{farm} variables R_D and θ is shown in **Error! Reference source not found.** for a case with three upwind turbines.

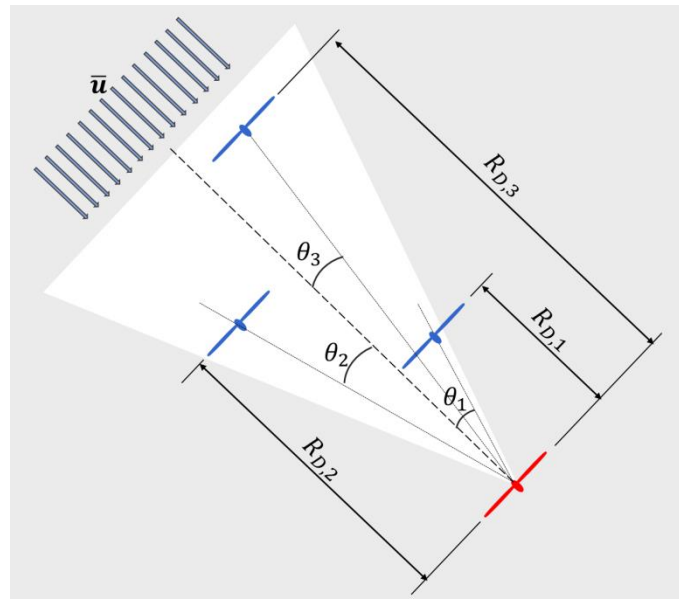


FIGURE 1.1 VARIABLES DESCRIBING RELATIVE POSITION OF UPWIND WIND TURBINES

A sample of the input variable space needs to be created in order to provide a list of inputs for the load simulations. Here, we follow the approach described in [11] and the sample space is filled by means of a Quasi-Monte Carlo simulation. Each variable is given a range (upper and lower bound) and is considered uniformly distributed within the bound and uncorrelated with other variables. For the turbulence, the bounds are conditionally dependent on the wind speed in order to account for the frequently observed wide range of variation of turbulence at low wind speeds. Then, the samples are generated using a Halton sequence, which provides pseudorandom numbers with low discrepancy, and results in a very uniformly filled sample space. An exception is the wind speed, which is modeled as a truncated Weibull distribution, with lower and upper bounds equal to the cut-in and cut-out wind speed. This choice is meant to compensate for the wider bounds of the turbulence at low wind speeds – meaning that if the wind speed was modeled with a uniform distribution, there would be more sparse coverage of the variable space at low wind speeds [11].

Sampling the wind farm-effect (wake) variables also requires special considerations. In the load simulations, the wake effects are taken into account with the help of the Dynamic Wake Meandering (DWM) model [16]. The load simulation software only simulates the loads on one turbine, while it can take multiple wake sources into consideration [17]. The most realistic way of using the DWM is to include the full wind farm geometry and thus treat all turbines as potential wake sources. Therefore, the following procedure is followed in creating each simulation input:

- 1) A random wind direction is sampled uniformly in the range (0,360) degrees.
- 2) A random wind turbine is picked out of the wind turbines in the wind farm under consideration. It is the turbine to be simulated, the remaining turbines are treated as wake sources
- 3) All turbines are assigned random de-rating level, uniformly distributed from 0 to 100%.
- 4) Random wind speed and turbulence realizations are generated
- 5) A Hawc2 load simulation is carried out with inputs defined in points 1-4.

- 6) All potential disturbing turbines are identified as turbines that are directly upwind or within an ± 20 deg angle from the wind direction
- 7) The distance, relative angle, and de-rating level of the M closest disturbing turbines are defined as features (variables) in the Machine Learning procedure used to train the surrogate model. Note that this "cut-off limit" M is only present in the surrogate model input feature set, the load simulations are always carried out while including all potential wake sources.

2. PROBABILISTIC MODELS FOR WIND FARM CONTROL

2.1. Probabilistic models

The wind turbine structure is designed to meet the mechanical loading corresponding to a given wind turbulence class. The fatigue lifetime of the blade, tower etc. is ensured based on the 90% quantile of turbulence for a selected turbulence class. While the turbulence for the rotor-nacelle-assembly (RNA) is typically designed based on the IEC specification (IEC 61400-1, 2005), the tower is designed to site-specific wind conditions. The uncertainties in the wind conditions can be relatively large, especially due to seasonal variations, storms and also changing terrain conditions over the life of the turbine. Thus measurement of turbulence on a continual basis, such as by the use of a spinner anemometer can be a valuable means for verifying that the turbulence is always below the design level or initiating control action for elevated turbulence levels. A means of supervisory control is curtailment of selected wind turbines in a wind farm, which is due to reduced power requirements from the grid. Curtailment can be made by selecting wind turbine locations that have high wake turbulence within the wind farm. The thrust from the wind turbine that is de-rated reduces and this leads to lower wake turbulence behind the de-rated turbine. This in-principle can reduce the fatigue damage on turbine components on the turbines in the wake. Reduction in fatigue leads to lower wear and larger life of the components.

Further de-rating of wind turbines should be made not by only reducing the power setpoint, but to do this through a combination pitch and rotor speed variation. If a derating is made in a time interval Δt and it reduces the failure rate from $\lambda_{baseline}$ to λ_{CS} (for example from 2 failures to 1 failure the time interval), the cost savings ΔC_{CS} of this strategy compared to a reference operation is:

$$\Delta C_{CS} = (\lambda_{baseline} - \lambda_{CS}) \cdot \Delta t \cdot C_{CM} \quad (2-1)$$

Δt is the time interval of the reduced failure rate and C_{CM} is the average cost for corrective maintenance. This may be directly quantified using the cost models developed in deliverable D2.1.

Based on available measurements, operational load cases can be simulated for the full wind farm, thereby determining the loads on all major wind turbine components across the wind farm. The details of the loads cases can be determined from the IEC 61400-3 standard. The problem statement is then posed as: Given the load case simulation results, determine the probability of failure of the wind turbine structure based on specific governing limit states:

2.1.1 ULTIMATE LIMIT STATE ANALYSIS.

For offshore wind turbines, the long term 10-minute extreme load value distribution over all operating mean wind speeds during normal operation is given by

$$F_{longterm}(l|T_{10min}) = \int_{V_{in}}^{V_{out}} \int_{H_{si}}^{H_{so}} F_{shortterm}(l|T_{10min}, v, \sigma_u) f(H_{s|v}) f_V(v) dH_{s|v} dV \quad (2-2)$$

Where $F_{shortterm}(l|T_{10min}, v, \sigma_u)$ is the short term extreme load at the mean wind speed v , turbulence σ_u with a ocean wave significant wave height $H_{s|v}$. For fixed base offshore wind turbines, the blades and other structures of the rotor nacelle assembly (RNA) are not affected by

ocean waves and therefore the waves terms in Eq. (2-2) are not considered for the RNA extreme loads, but only for the support structure.

The corresponding annual probability of the extreme load value is

$$F_{longterm}(l|T_{1year}) = F_{longterm}(l|T_{10min})^N \quad (2-3)$$

where N is the expected number of statistically independent 10-min periods in one year under normal operation

Equation, 2-2 and 2-3 are with respect to the extreme load level. However to determine the probability of failure, it is necessary to connect this to the ultimate limit state of the structure.

For example, the ultimate limit state at the tower base is given by

$$G = Y_{cr}X_R - L_{ULT}(\sigma_u, v)X_{sim}X_{exp}X_{aero}X_{str} \leq 0 \quad (2-4)$$

Where Y_{cr} is the design load criteria, L_{ULT} is the extreme load value with the probability $F_{longterm}(l|T_{1year})$, X_R is the uncertainty in the material parameter, X_{sim} is the simulation uncertainty, X_{exp} is the exposure or environmental uncertainty, X_{aero} is the aerodynamic coefficient uncertainty and X_{str} is the structural parameter uncertainty. The structural reliability of the tower (for example as a result of the extreme tower bottom extreme fore-aft bending moment) is then assessed based on different wake situations, with and without de-rating. An acceptable reliability index is $\beta \geq 3.3$ corresponding to an annual probability of failure $p_f \leq 5 \cdot 10^{-4}$.

2.1.2 FATIGUE LIMIT STATE ANALYSIS.

The damage to turbine structures is estimated based on Miner's rule for linear damage accumulation and the limit state equation is written based on an appropriate SN curve for the structure that is being assessed.

$$g(t) = \Delta - \int_{v_{in}}^{v_{out}} \int_{\sigma_{ui}}^{\sigma_{uf}} n \cdot \frac{t}{K} X_{wind}^m D(m, v, \sigma_u) f(\sigma_u|u) f(v) d\sigma_u dv \quad (2-5)$$

where n is the number of stress cycles with damage D over mean wind speed v at a turbulence of σ_u with SN curve slope of m , and γ -intercept of K , X_{wind} is the uncertainty in the wind and Δ is a stochastic variable describing the model uncertainty related to Miner's rule. The design lifetime is chosen to be 25 years. The annual probability of failure in year t is estimated by:

$$\Delta P_F(t) = \frac{P(g(t) \leq 0) - P(g(t - \Delta t) \leq 0)}{1 - P(g(t - \Delta t) \leq 0)} \quad (2-6)$$

The accumulated reliability index $\beta(t)$ is defined from the accumulated probability of failure by:

$$\beta(t) = -\Phi^{-1}(P_F(t)) \quad (2-7)$$

where $\Phi(\cdot)$ is the standard normal distribution function. The corresponding annual reliability index is denoted $\Delta\beta$ and should be ≥ 3.3 . The fatigue damage evaluation is made cumulatively year after year and the year t at which $\Delta\beta$ falls below 3.3 is taken as the design life. Therefore if it is assumed that the Lillgrund wind farm is design for 25 years with a $\Delta\beta$ at 3.3 in year 25, then it should be shown that with de-rating the resulting damage allows for extending the life by X years for the same reliability index in the last year or that the reliability in year 25 is increased. Life extension of the wind farm results in increased energy capture while improved reliability leads to reduced maintenance costs, both of which reduce the LCOE.

2.2. Design Limits

In terms of design limit states, the fatigue design limit state in Eq. (2-5) is often measured using the concept of damage equivalent loads, that is equivalent load that results in the total number of load cycles experienced by a component in its lifetime. The damage equivalent fatigue load, L_{eq} given a load time series, L_i with n_i cycles and a reference number of cycles in its lifetime of N_{ref} is calculated using the formula

$$L_{eq} = \left(\frac{\sum n_i L_i^m}{N_{ref}} \right)^{\frac{1}{m}} \quad (2-8)$$

The number of load cycles depends on the operating conditions of the wind turbines and the Weibull probability distribution if mean wind speed over the period of operation. Since fatigue of key structural components is correlated to wind turbulence, it is beneficial to the turbine life, if the curtailment that is made, is at locations within the farm so as to reduce high wake turbulence. The line of turbines corresponding to B-8, C-8 and D-8 in Lillgrund as shown in Fig 2-1 is used to quantify the effects of de-rating.

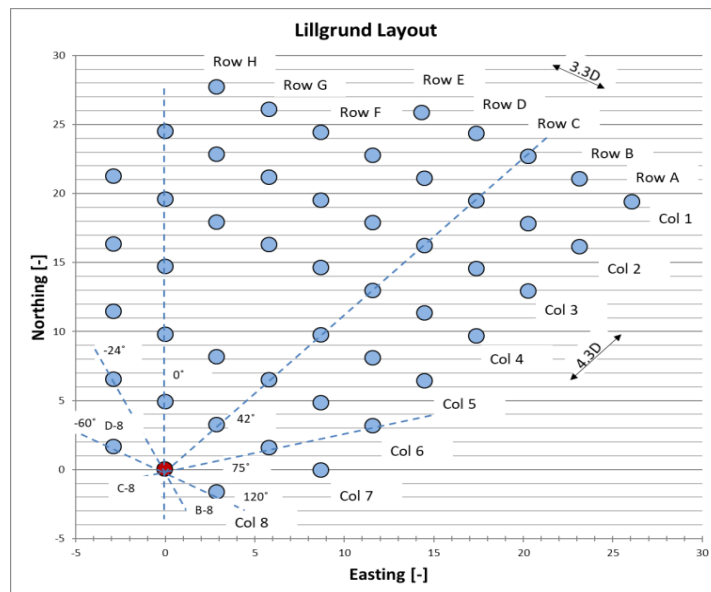


FIGURE 2.1: LAYOUT OF THE LILLGRUND WIND FARM

Based on changing the pitch set-point of the turbine B-8 when the incoming wind direction is at 120 degs, one can determine the load reduction level feasible in the downstream wind turbines, Co8 and D-8. The upstream turbine is de-rated and the effect of a reduced thrust on the upstream turbine is evaluated on the downstream turbines. Figure 2.2 displays the reduction in the blade root flap damage equivalent moments at different mean wind speeds. It can be that the observed reduction in loads is much more and consistent for the turbine just behind the de-rated upstream turbine, that is C-o8 has systematic reduction in loads over most wind speeds than the turbine further downstream D-o8. It is also observed that greater reduction in loss is observed on Co8 with higher de-rating or increased pitch setting of the upstream wind turbine.

Therefore de-rating has a direct impact on the fatigue design limit, by reducing the damage equivalent load level. De-rating can also impact the extreme design limit for operating load cases, since the wake turbulence is reduced. So all extreme loads as per Eq. (2-2) which are directly proportional to the wind turbulence level can be reduced through de-rating. However if the extreme limit state is governed by non-operational cases such as idling under storms or shut-downs under grid loss events etc., then the effect of de-rating will not be seen on the extreme limit states as these situations are not influenced by de-rating. Therefore the remaining sections of this document mainly focus on the fatigue design limit state.

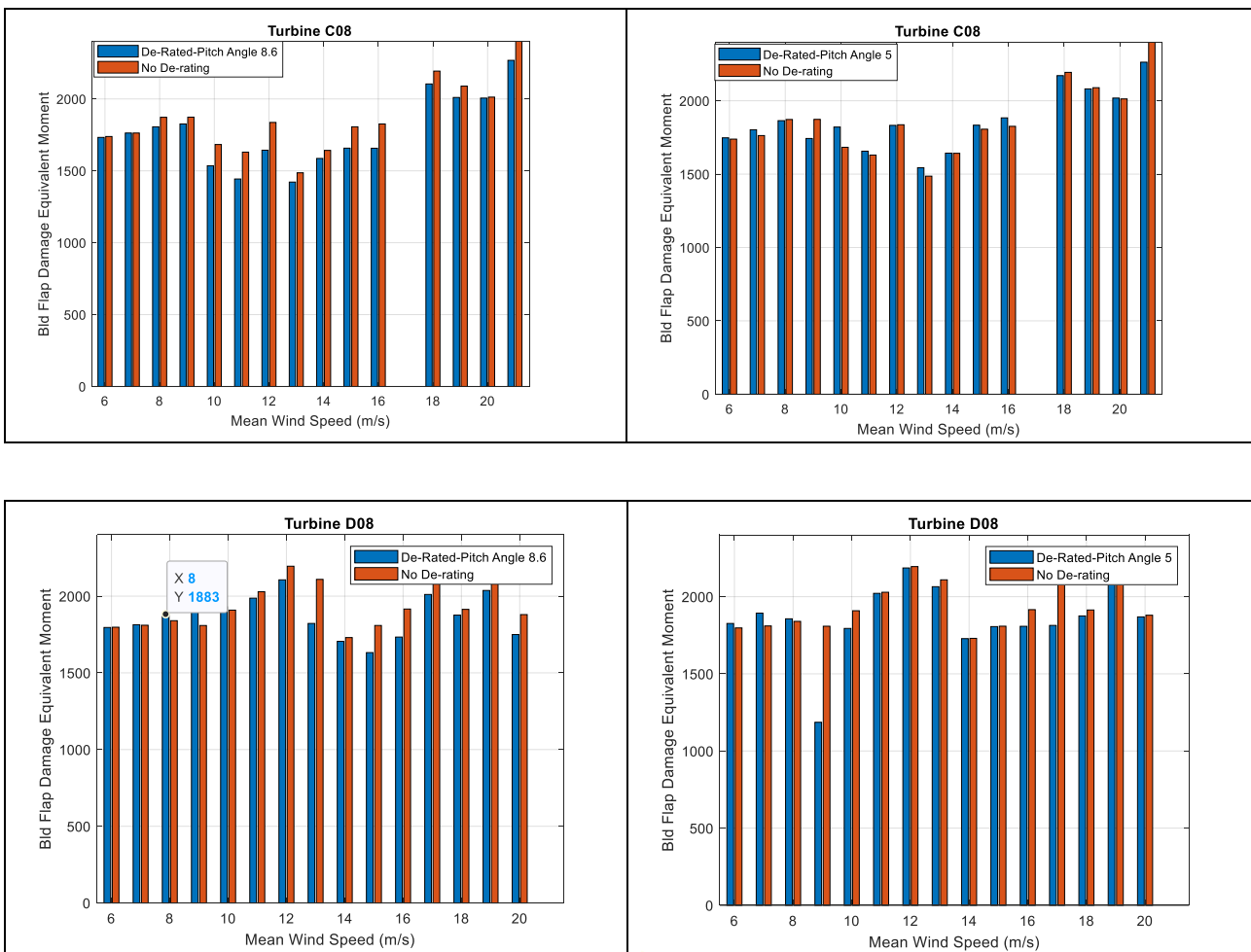


FIGURE 2.2: LOAD REDUCTION AT THE BLADE ROOT ON DOWNSTREAM TURBINES DUE TO DE-ARTING UPSTREAM TURBINE, HIGHER DE-RATING IS OBTAINED BY INCREASING THE BLADE PITCH ANGLE SETTING

2.3. Remaining Life Estimation

While the duration of curtailment needs to be decided, even a 20% reduction in damage equivalent moments at the blade root with just 10% of the total time in de-rating of the upstream wind turbine can result in a significant improvement in the lifetime of the blade of at least 15 years. This is because the fatigue life (SN) curve of the blade has a large exponent of 12 which translates even a small load reduction into a large increase in lifetime. Similarly for the same load reduction, the support structure life could be extended by 6 years since it has an SN curve slope of 5. Curtailment of power, while reducing the power on the turbine, that is de-rated actually increases the overall output of the wind farm due to reduced wake effects, so long as only the leading wind turbines are curtailed. This implies that we obtain longer life of the farm and increased energy production simultaneously. Since the increase in energy capture has a 1:1 correlation to reduction in LCOE, the simple strategy of de-rating the leading turbine in a row of wind turbines can lead to significant reduction in LCOE, which is quantified in section 5.

2.4. Baseline Case at Lillgrund

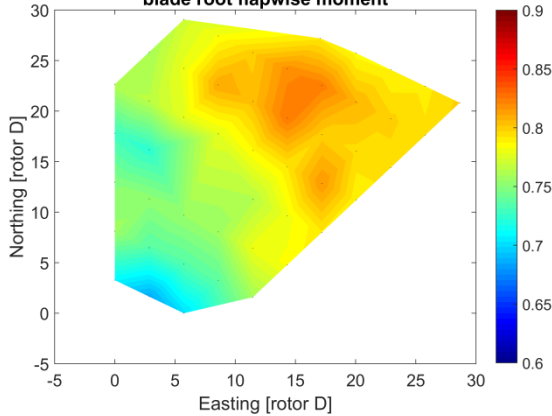
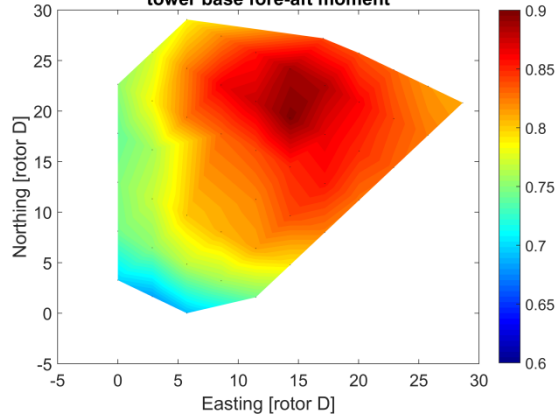
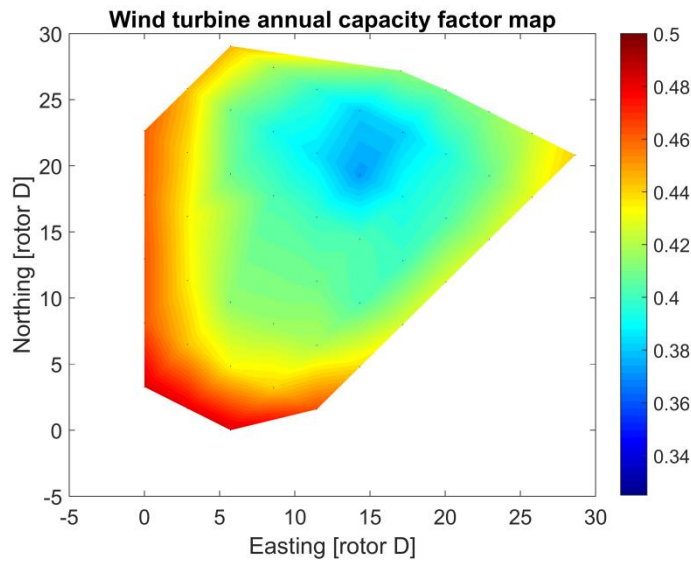
In order to evaluate any potential benefit of advanced control strategies, a reference needs to be established in terms of both Annual Energy Production (AEP) and fatigue lifetime. Since for most wind farms all wind turbines in the farm have identical rotors, it can be assumed that the fatigue capacity for rotor components corresponds to a standard reference wind class. The turbine type installed at Lillgrund is certified for wind class 1A, which is also the class used in the present report. The support structures (foundation and tower) may differ within an offshore wind farm: as a minimum, the foundation properties will vary due to the different depth at which turbines are installed; towers may also be tailored to the specific turbine position. Therefore, unless the actual design specifications of each support structure are known, it is impossible to define a reference load level or wind class for the support structures. An alternative is to consider that all support structures are tailored to satisfy a criterion for minimum reliability, by carrying out individualized design load calculations. As we currently do not have this information, we assume that the support structures also satisfy the design criteria for an IEC 1A reference class.

The lifetime-equivalent loads and power output at each turbine are estimated by sampling the predictions of the surrogate model over the site-specific distributions of environmental conditions: wind speed, turbulence, and wind direction. The sample points form a 3-dimensional, rectangular, evenly spaced grid, and the relative weight of each sample point is computed from the joint site-specific probability distributions of wind speed, turbulence and wind direction. All distributions are obtained based on approx. 3 years of SCADA records of the full wind farm. The procedure to determine the joint distribution of environmental conditions from SCADA is described in [12]. The actual distributions used in the present report are given in Table 2.. For each sample set of environmental conditions, the load and power surrogate model is evaluated for each turbine in the wind farm. As the model requires inputs regarding the relative position of upwind turbines, these are determined for each sample based on the wind farm geometry and the wind direction. The surrogate model outputs are then weighted according to the joint probability distribution of wind speed, turbulence, and wind direction. As a result, an estimate of the lifetime equivalent DEL (Damage-Equivalent Loads) as well as annual power capacity factor are obtained. The load estimates are then normalized with respect to the lifetime-equivalent loads for wind conditions

corresponding to IEC class 1A, computed using the same surrogate model which provides the site-specific load estimates. The resulting lifetime-equivalent load maps for blade root and tower base are shown on Figures Figure 2.3 and 2.4 respectively, while Figure 2.5 shows the map of the estimated annual power capacity factor over the wind farm.

TABLE 2.1 PROBABILITY DISTRIBUTIONS OF ENVIRONMENTAL CONDITIONS AT LILLGRUND

Parameter	Wind direction θ (center of a 30deg bin)											
	0°	30°	60°	90°	120°	150°	180°	210°	240°	270°	300°	330°
<i>Prob</i> (θ)	0.0078	0.0523	0.053	0.0694	0.0742	0.0908	0.0693	0.1298	0.1554	0.1406	0.0799	0.0776
Weibull <i>A</i>	9.8983	7.2201	7.6999	8.0805	9.728	9.0413	8.5406	9.9078	10.263	10.533	9.8033	7.5229
Weibull <i>K</i>	2.3092	2.1077	2.3226	2.4469	2.6137	2.4477	2.2307	2.3793	2.5309	2.4411	2.1822	2.0217

Lifetime-equivalent DEL compared to IEC class 1A reference, blade root flapwise moment

FIGURE 2.3 LIFETIME EQUIVALENT BLADE FLAPWISE BENDING MOMENT DEL VARIATION MAP
Lifetime-equivalent DEL compared to IEC class 1A reference, tower base fore-aft moment

FIGURE 2.4 LIFETIME EQUIVALENT TOWER BASE FORE-AFT BENDING MOMENT DEL VARIATION MAP

FIGURE 2.5 ANNUAL CAPACITY FACTOR MAP FOR THE LILLGRUND WIND FARM

3. LOAD ALLEVIATION USING SURROGATE MODELS

The procedure described in section 1.1 is used to generate random scenarios from two hypothetical wind farm geometries and with the actual geometry of the Lillgrund wind farm (Figure 3.1). A total of 10,000 samples are generated with each wind farm geometry, leading to 30,000 different combinations of environmental conditions and wake-induced effects.

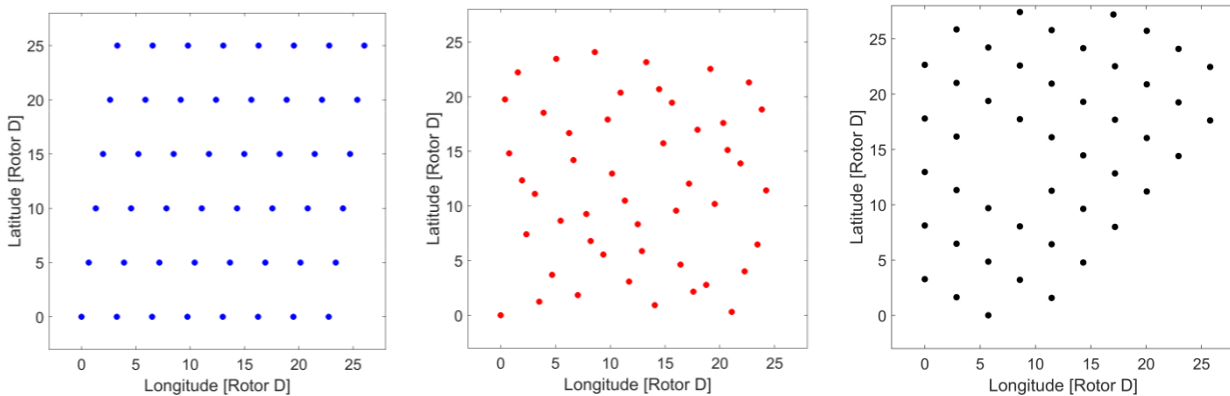


FIGURE 3.1 WIND FARM GEOMETRIES USED IN LOAD SIMULATION DATABASE CREATION. LEFT: "REGULAR" WIND FARM; CENTER: "CHAOTIC" WIND FARM, RIGHT: LILLGRUND WIND FARM

For each sample point, six load simulations with different turbulence realizations are carried out using the Hawc2 aeroelastic simulation software [13]. The multiple turbulence seeds per sample point are used in order to take into account the statistical uncertainty arising from the the realization-to-realization difference in the turbulent wind fields. For each realization, the load analysis simulates the response of a single turbine subject to wake-induced effects from all remaining turbines in the wind farm. All six realizations at a given sample point simulate the same, single, randomly chosen wind turbine from the wind farm. The wind turbine numbers to simulate for each sample point are drawn from the uniform distribution, meaning that there is an approximately equal number of simulations corresponding to each wind turbine position in the wind farm.

The end result is 180,000 simulations covering a range of environmental conditions, de-rating levels, wake-induced effects in a wind farm, and accounting for realization-to-realization uncertainty.

3.1. Fitting procedure and validation of load and power predictions at Lillgrund

A surrogate model for prediction of fatigue loads and power outputs is trained based on the load simulation set described above. The model chosen is a feed-forward Artificial Neural Network (ANN) with three hidden layers. The input feature vector is assembled following the procedures described in Section 1.2:

- As there are six simulations with different turbulence seeds for each combination of environmental conditions, all outputs (damage-equivalent fatigue loads and power) are

taken as the average of the results from the six realizations. Each row in the input feature vector corresponds to one sample point, meaning a total of 30,000 input data rows are available for model training;

- The features included in the training represent 1) environmental conditions: free wind speed, turbulence and wind shear – describing undisturbed wind conditions, 2) for each upwind turbine, two features describing the distance to the upwind turbine in rotor diameters, and the relative angle between the wind direction and the direction of the upwind turbine. Up to five of the closest upwind turbines are considered, leading to ten features related to the description of wake-induced effects. The upwind turbines to be included as features are chosen as the closest five turbines in a direction within a range of ± 20 deg from the free wind direction.

Using the feature set described above, a single ANN model is trained to predict all outputs simultaneously by having an output layer with size equal to the number of outputs (Figure 3.2). The model training is carried out using standard back-propagation with the Adam algorithm.

A script is developed which based on the farm geometry and a given free wind direction, automatically derives the features describing the wake-induced effects for each turbine in the wind farm. As a result, by only specifying free-wind conditions: wind speed, turbulence, wind shear and wind direction, the load and power outputs for each turbine in the wind farm are computed automatically with the surrogate model.

Three years of SCADA records (power, pitch and rpm values) for all turbines at Lillgrund are available, as well as blade root load measurements for a few months on a single turbine (C-8, see Figure 2.1). It is therefore possible to validate the predictions of the surrogate model described above: the power predictions can be validated against measured power signals from SCADA on all turbines, while the blade root flapwise fatigue predictions can be validated at turbine C-8. For this purpose, the SCADA data are filtered and the free wind speed and turbulence are estimated based on the procedure described in [12] (as also discussed in Section 2.1). The free wind speed and turbulence are then given as inputs to the surrogate-based prediction model, and as a result the power output of each turbine is predicted for every 10-minute period in the SCADA records.

The feature set used to train the simulation-based surrogate model is designed in a way that the simulation outputs can also be replaced by SCADA-based measurements, meaning that a purely data-driven model can also be trained using the same model architecture (Figure 3.2).

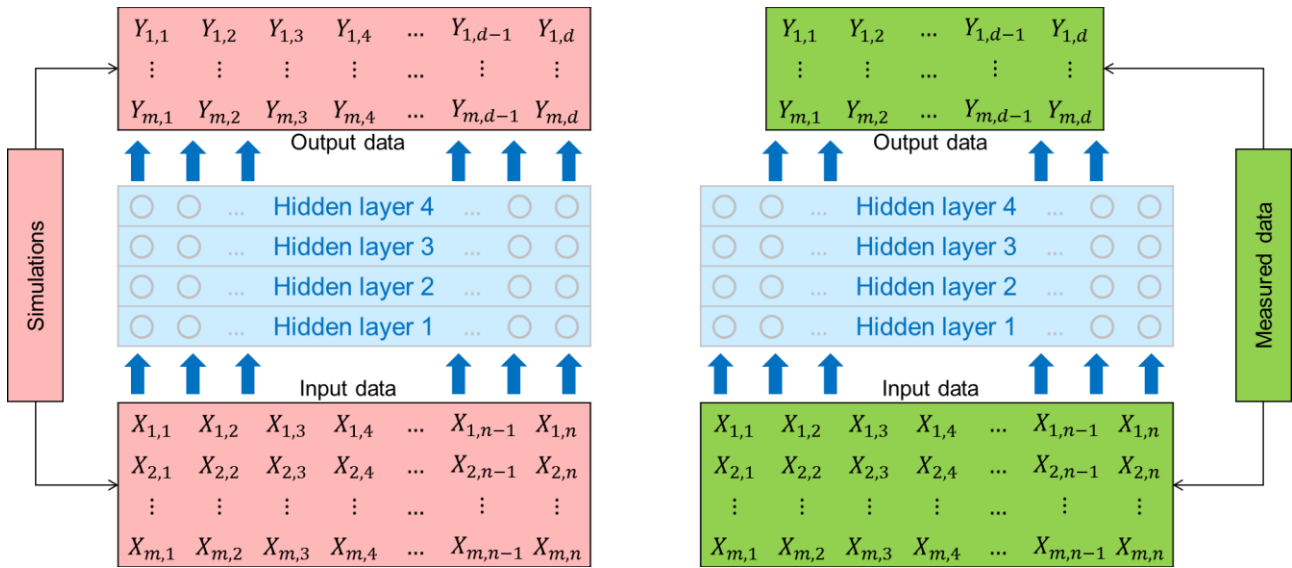


FIGURE 3.2 SURROGATE MODEL TRAINING SETUP, WHERE BOTH SIMULATIONS AND DATA CAN BE USED AS INPUTS FOR A MODEL WITH THE SAME ARCHITECTURE.

Since the power output is available in the SCADA records for all turbines at Lillgrund, a purely data-driven power prediction model is also trained. As a first check on the validation accuracy, the total wind farm power output (i.e., the sum of individual turbine outputs) predicted by both the simulation-based and by the data-driven models is compared to the actual farm power output (Figure 3.3).

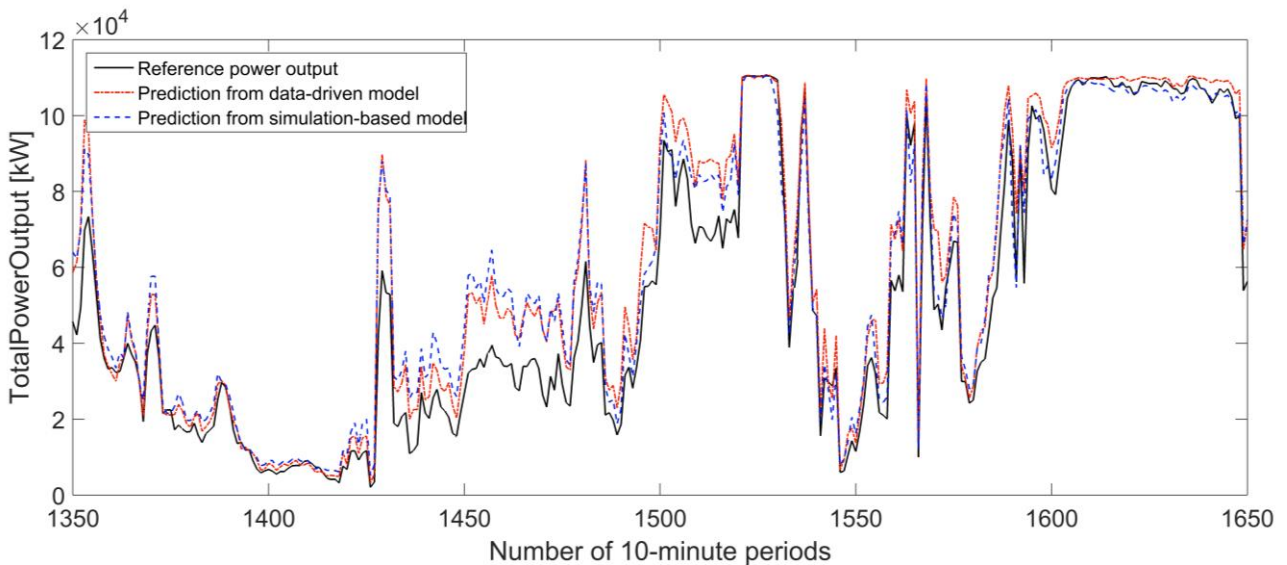


FIGURE 3.3 TOTAL POWER OUTPUT PREDICTION AT LILLGRUND

Then, to compare the predictions of different models for a specific case, the power output is simulated for the case of gm/s free wind speed with wind direction 220deg as shown in Figure 3.4. This is a specially challenging case due to the wind coinciding with turbine row orientations, leading to strong wake effects.

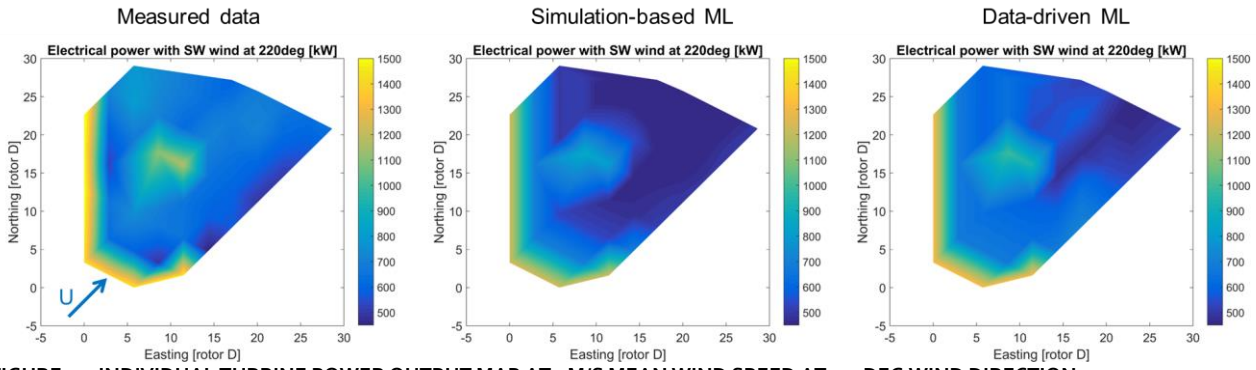


FIGURE 3.4 INDIVIDUAL TURBINE POWER OUTPUT MAP AT 9M/S MEAN WIND SPEED AT 220DEG WIND DIRECTION

Clearly both the simulation-based and data-driven models show that they capture the variation in power output in the wind farm. For a more general comparison, Figure 3.5 shows the r-squared and rms-error between measured wind turbine power outputs and the predictions from the simulation-based surrogate model. Finally, the blade root flapwise damage-equivalent fatigue loads are predicted for the turbine equipped with load measurement instrumentation, and simulation results are compared with the measurements on Figure 3.6. To the extent that it can be judged from a single turbine and a single load channel, the load predictions from the simulation-based surrogate model also show reasonable accuracy, and also show the capability of the model to predict the occurrence and extent of wake-induced load increases.

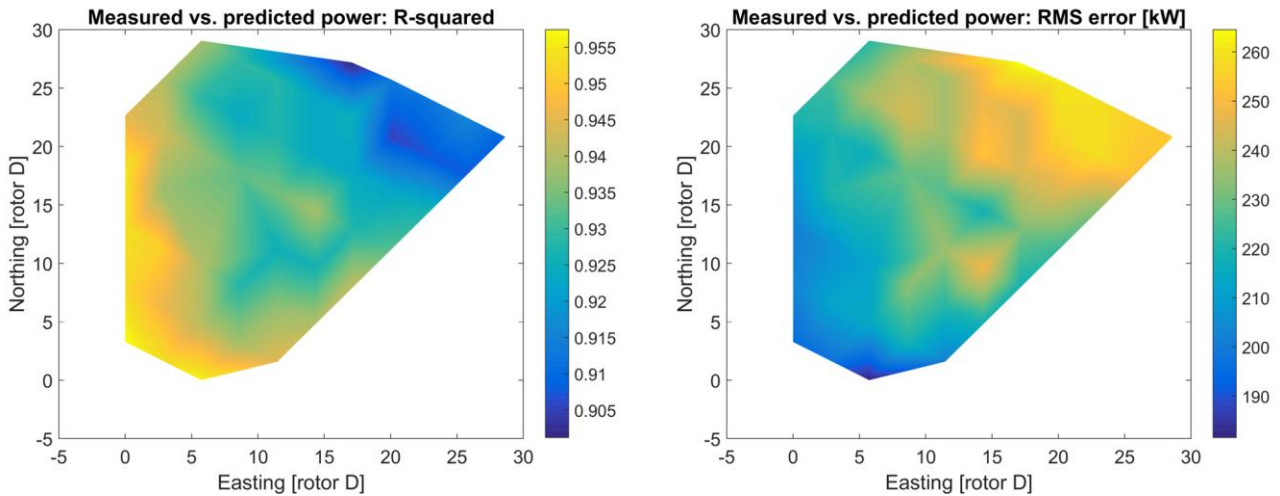


FIGURE 3.5 ACCURACY MAPS FOR POWER PREDICTIONS OF INDIVIDUAL TURBINES AT LILLGRUND

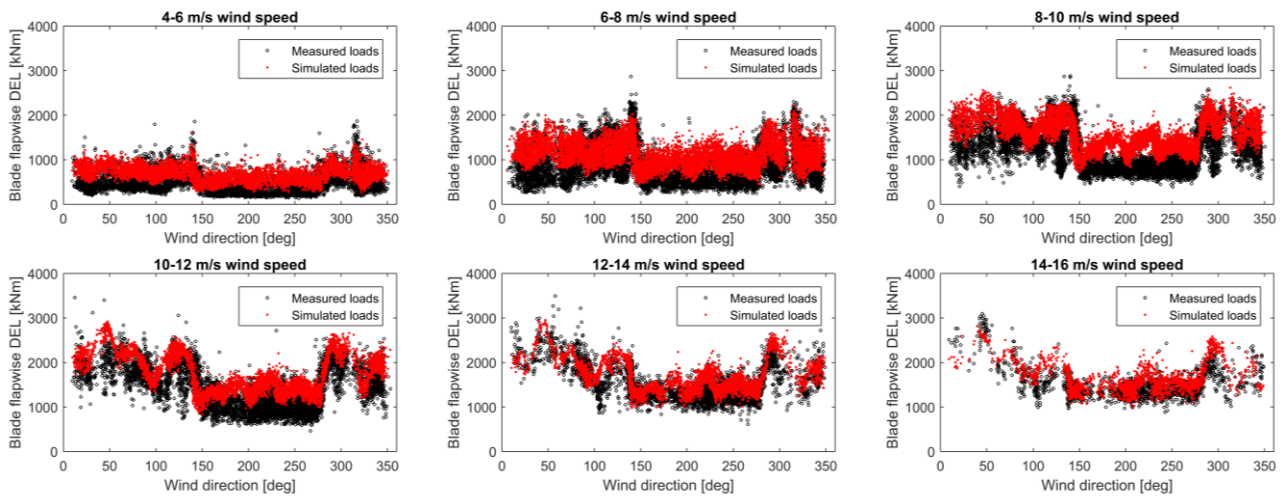


FIGURE 3.6 BLADE FLAPWISE FATIGUE LOADS AT TURBINE C-08 AT LILLGRUND: COMPARISON OF SIMULATIONS WITH DATA

Using the same approaches but with additional load simulations, the surrogate model is expanded to cover scenarios including de-rating as a control strategy – considering derating on both on the turbine being analysed, and on upwind turbines acting as wake disturbance sources. The results of the use of this expanded surrogate model are presented in Section 4.2.

4. WIND FARM PERFORMANCE FOR TARGET RELIABILITY

This chapter presents models for estimating degradation and lifetime of power converters and transformers. The degradation and lifetime models presented result directly in an estimate of the lifetime, remaining lifetime or consumed lifetime.

4.1. Predicted annual reliability under operating conditions

Evaluating the consequences of choosing a specific wind farm operating strategy requires the computation of summary measures of wind farm and turbine performance over the entire lifetime such as power output, lifetime-equivalent fatigue loads, or costs. The structural reliability index is a useful choice for this purpose as it provides a summary measure, which accounts simultaneously for variations in loads exposure and for uncertainty. In terms of finding an optimal control strategy, the reliability can be utilized by setting a target reliability index as a constraint for each turbine in the farm, and running an optimization procedure with power output, cost, or other utility measure as an objective. A successful optimization will yield a fairly uniform reliability over the wind farm, meaning that the loading at each turbine is the maximum allowable within the tolerable limits.

The most critical limit state for considering in performance optimization is fatigue as it accumulates the long-term effects of any changes in the control strategy. We therefore focus on fatigue as a primary limit state for considering with reliability analysis. The following limit state is considered (a modification from eq. 2-5, now using damage-equivalent loads (DEL) instead of fatigue damage):

$$g(t) = S_{mat}(t) - X_{exp}X_{sm}X_{stat} \int_{\theta} p(\theta|t)S_{eq}(\theta)d\theta \quad (4-1)$$

where t is a reference time period, θ is a manifold of variables describing external conditions included in the model (presently wind speed, turbulence and wind direction) which have a joint probability of $p(\theta)$, $S_{eq}(\theta)$ is the damage-equivalent fatigue load for a specific combination of external conditions θ , S_{mat} is the limit damage-equivalent load which would lead to the turbine (component) failing after exactly one time period t . X_{exp} , X_{sm} , X_{stat} are uncertainty variables which are described in details in table 4.1.

TABLE 4.1 DESCRIPTION OF UNCERTAINTY VARIABLES INCLUDED IN RELIABILITY MODEL

Variable	Mean	c.o.v	Distribution	Description
X_{exp}	1	0.05	Gaussian	Accounting for uncertainty in estimating the exposure to environmental conditions, e.g. wind and waves
X_{sm}	1	0.05	Gaussian	Model uncertainty due to the use of a surrogate model which has certain limitations in accuracy
X_{stat}	1	0.01-0.03	Gaussian	Statistical uncertainty accounting for seed-to-seed variations in load simulations results which mean that estimated lifetime loads will be uncertain if a finite number of simulations are used. The coefficient of variation is different for different load channels.

Reliability estimates obtained from structural reliability analysis are very sensitive to the choice of uncertainty model. Hence, the reliability models are most suitable for comparison tasks, and in order to draw robust conclusions, it is necessary to establish a reference, baseline reliability model, to which other reliability estimates can be compared. In the present case, we establish a reference reliability model by calibrating the value of a Weibull-distributed “material strength” S_{mat} so that equation 4-1 yields a reliability index of $\beta_{ref} = 3.3$ for loading conditions corresponding to IEC class 1A (defined in terms of the load variable S_{eq} and the external conditions variable vector θ). The calibration procedure is as follows:

- A reference material safety factor γ_m is selected (e.g. $\gamma_m = 1.5$)
- A target value for the coefficient of variation of S_{mat} is chosen, COV_{target}
- Given the safety factor and the coefficient of variation, a solution for Weibull distribution parameters A and k is sought so that a Weibull-distributed variable with these parameters will have the target coefficient of variation and its 5% quantile value will equal the mean divided by γ_m .
- A reliability analysis is carried out using the estimated distribution of S_{mat} , to find the reference reliability index
- Steps 2-4 are repeated with varying values of COV_{target} until the resulting reliability index equals the target reliability index of $\beta_{ref} = 3.3$

The resulting distributions are depicted in Fig. 5-1. This procedure ensures consistency with the deterministic design equations used by e.g. the IEC61400-1 standard, which define the design in terms of material and load safety factors and characteristic material strength and characteristic load values. The typical characteristic material strength is taken as the 5% quantile of the material strength distribution, hence the use of the 5% quantile in the calibration.

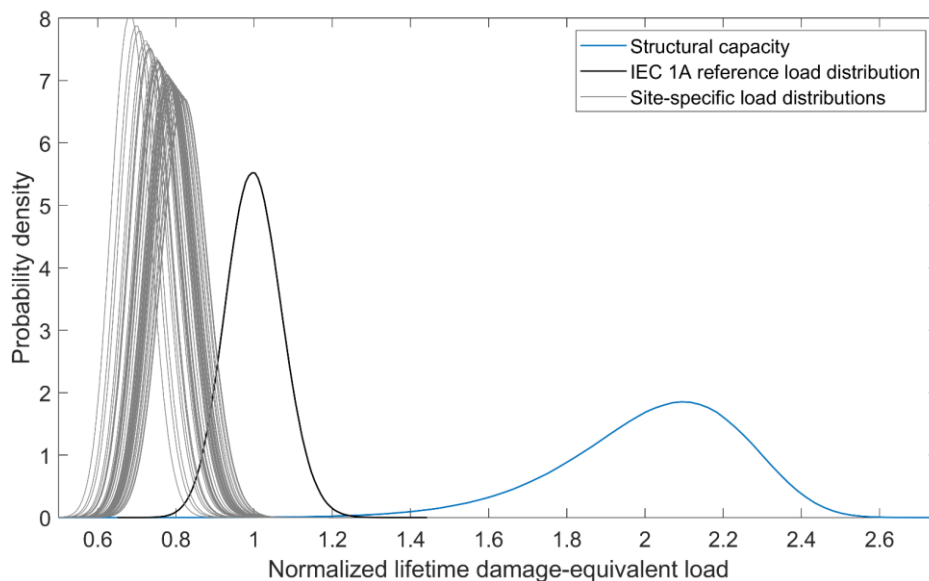


FIGURE 4.1 LIFETIME-EQUIVALENT LOAD DISTRIBUTIONS FOR INDIVIDUAL TURBINES AT LILLGRUND COMPARED TO IEC1A REFERENCE

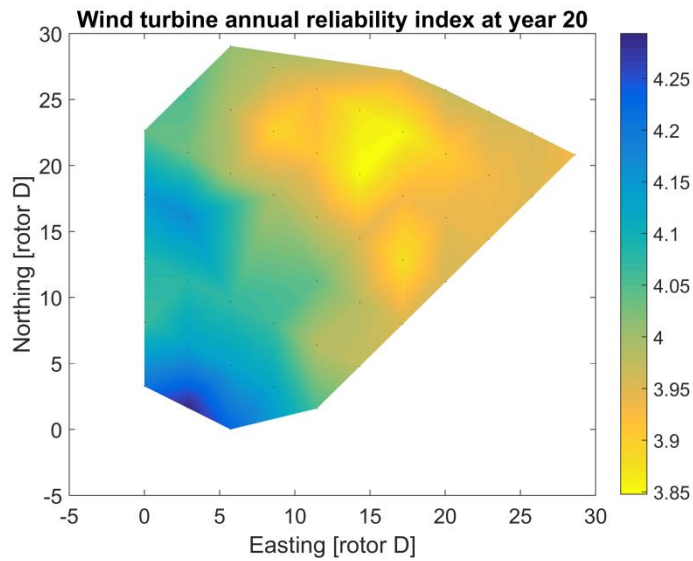


FIGURE 4.2 RELIABILITY INDEX MAP FOR BLADE ROOT FLAPWISE FATIGUE AT LILLGRUND UNDER NOMINAL CONDITIONS (NO DERATING)

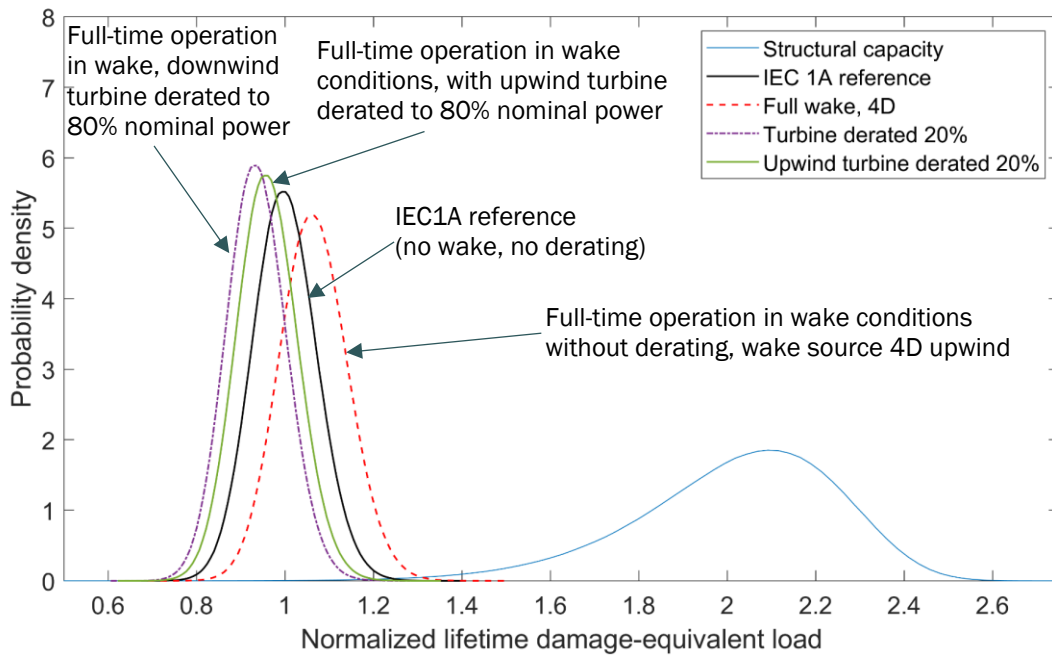


FIGURE 4.3 COMPARISON OF FATIGUE LOAD DISTRIBUTIONS FOR DIFFERENT CONTROL SCENARIOS FOR A TURBINE SUBJECTED TO WAKE DISTURBANCE

4.2. Performance optimization

While full-fledged performance optimization is beyond the scope of this deliverable, we illustrate how the load and power modeling techniques presented here will provide the information necessary for performance optimization, which is to be demonstrated later in the project. For this purpose, we consider the example scenario at Lillgrund discussed earlier, with mean wind speed of 9m/s and wind direction of 220deg, with 10% turbulence intensity and wind shear exponent of 0.1. This wind direction, combined with the Lillgrund wind farm geometry, results in significant wake effects. As shown in Figure 4.4, left (and also Figure 3.5), under these conditions the turbines operating in free wind have large power production. However, there is a sharp drop in the production for all turbines further downwind due to the alignment between turbine rows and the wind direction which represents close to a worst-case scenario for wake-induced power losses. Using the surrogate-model approach described in sections 1.2. and 3.1, the wind farm power production and loads can be mapped for any combination of de-rating options for all the turbines in the farm. This allows us to explore various scenarios regarding the distribution of power production and load accumulation. The base hypothesis is that de-rating turbines close to the wind farm edge will allow more energy to reach turbines deeper in the farm, and the power output gains for the latter will compensate for the losses due to de-rating the front rows. An obvious first scenario is to de-rate the first row (only turbines in free wind). However, calculations with this scenario showed no net gain in power output: a turbine operating in free wind extracts energy in a close to optimal way, and de-rating these optimally operating turbines leads to net power loss in our calculations, regardless of how the downwind turbines are operated. As an alternative scenario, de-rating the second row of turbines (first row downwind from the edge of the wind farm) by 20% was investigated. This scenario showed some potential operational gains: the power losses in the second row seem to be compensated by power gains deeper in the wind farm (3rd row and further downwind) (Figure 4.4, right). Blade and tower fatigue loads on the second row increased, however they are lower or unchanged for all other turbines downwind (Figure 4.5). The relative change in power output and blade root flapwise fatigue loads is illustrated in Figure 4.6. In this particular scenario (combination of wind speed and wind direction), de-rating the second row of turbines by 20% resulted in estimated 4% increase in the total wind farm power output, while the total accumulated blade fatigue (estimated as the sum of the individual damage-equivalent fatigue load estimates over the entire farm) was reduced by approximately 3%. When expanding the scenario to cover other wind directions and wind speeds, it was seen that a net power gain is observed for wind directions within about ± 12 deg from the wind turbine row alignment, and for wind speeds in the range of 5-13m/s. These figures, together with considering the joint wind speed and wind direction distributions at Lillgrund, result in an estimated overall AEP gain of 2% as a result of applying the derating strategy.

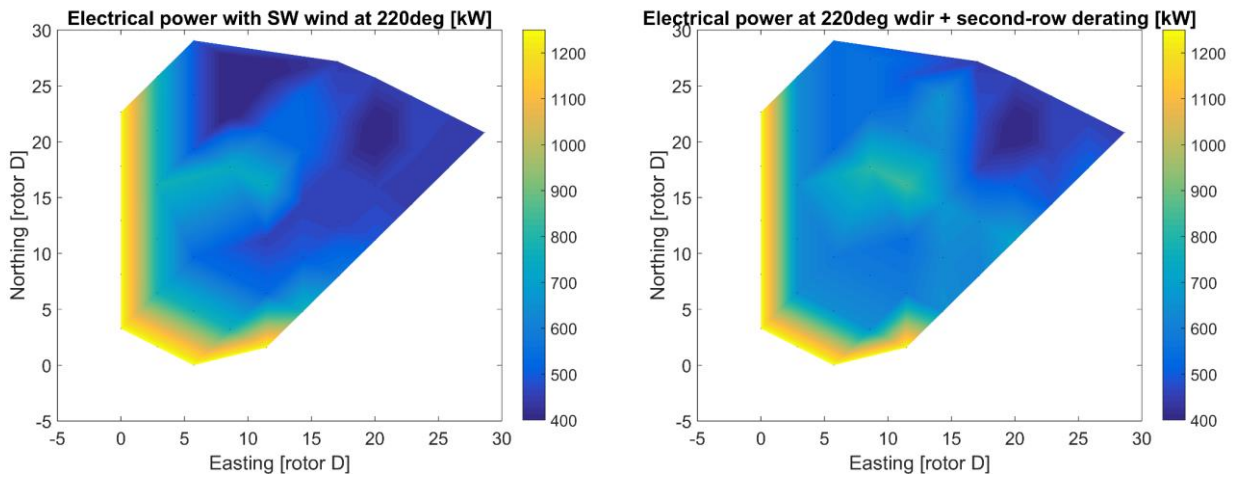


FIGURE 4.4 ILLUSTRATION OF THE EFFECT ON POWER OUTPUT ACHIEVED BY APPLYING 20% DE-RATING ON THE SECOND ROW OF TURBINES IN DOWNWIND DIRECTION

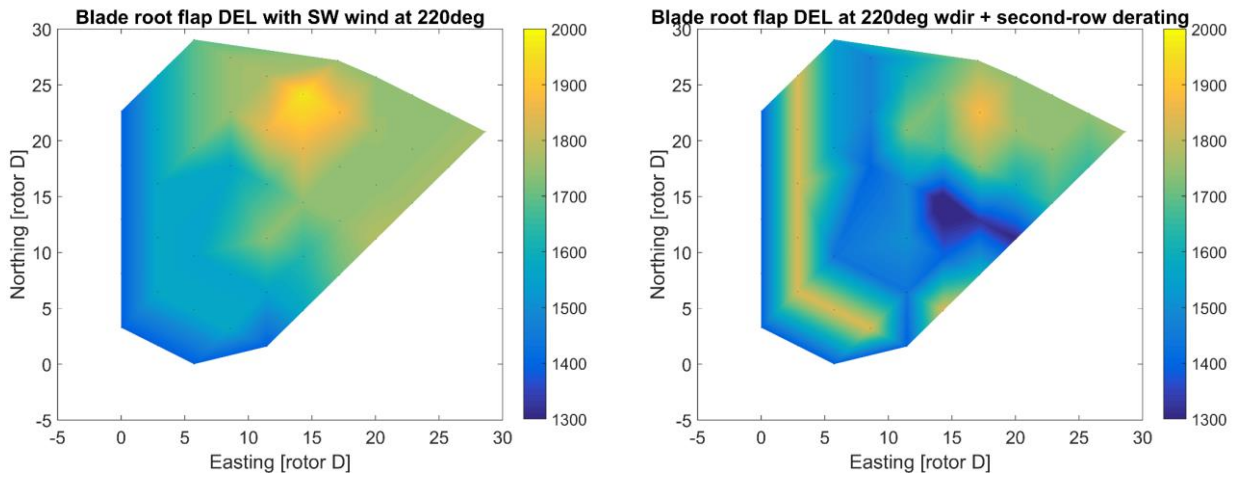


FIGURE 4.5 ILLUSTRATION OF THE EFFECT ON BLADE FATIGUE LOADS ACHIEVED BY APPLYING 20% DE-RATING ON THE SECOND ROW OF TURBINES IN DOWNWIND DIRECTION

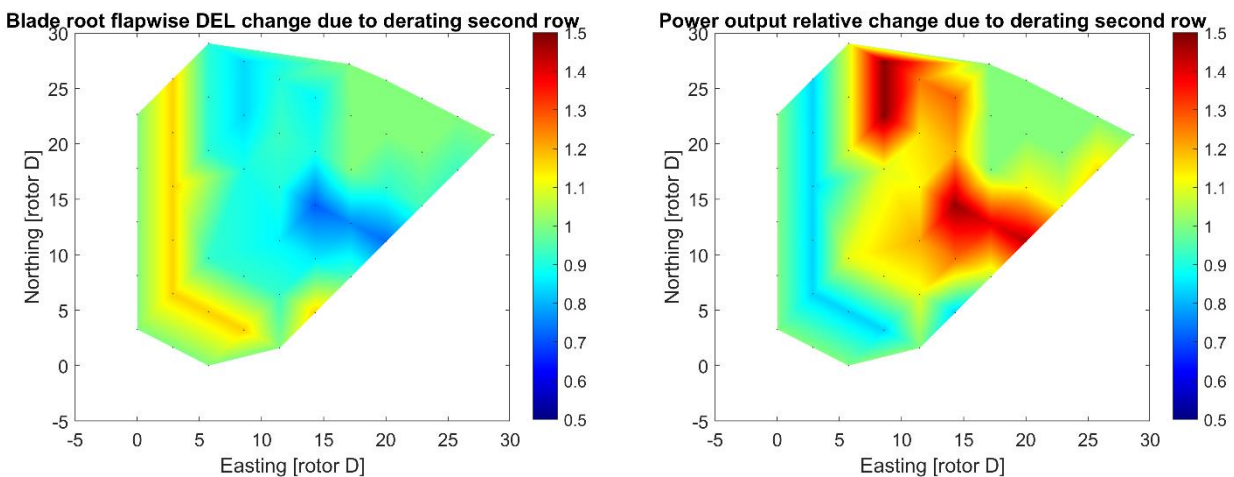


FIGURE 4.6 RELATIVE CHANGE IN WIND TURBINE LOADS AND POWER OUTPUTS OVER THE LILLGRUND WIND FARM DUE TO APPLYING 20% DE-RATING ON THE SECOND ROW OF TURBINES IN DOWNWIND DIRECTION

5. WIND FARM COST IMPACT

From the previous sections, it can be seen that the wind farm control influenced the farm energy capture performance, either at the individual turbine level (such as derating) or at the farm level (such as by reduced wake losses). Secondly, was the ability to reduce the wear of structures through reduced wake turbulence, which potentially lowers the maintenance costs and reduces downtime.

The failure rate for the baseline control strategy, $\lambda_{baseline}$, can be obtained from failure rate statistics or from a fatigue life degradation model using wind farm load simulations. The failure rate using a de-rating strategy, λ_{CS} , can be calculated by adjusting the baseline failure rate with a failure rate adjustment factor ε :

$$\lambda_{CS} = \varepsilon \cdot \lambda_{baseline} \quad (5-1)$$

ε is a factor that describes the relative change in number of failures or change in fatigue life degradation with de-rating as compared to the baseline situation. This approach is justified so long as the component failures are due to dynamic loading on the wind turbine and thereby the control strategy can influence the failure rate directly by affecting the dynamic loads. There are component failures that can occur due to other reasons such as manufacturing defects, improper operation such as use of wrong oil within a gearbox etc., which occurrences are not considered herein as they are not directly correlated to dynamics loads or control actions.

For load-influenced failures, if the failure is measured in terms of fatigue life degradation, then the failure rate in Eq. 5-1 is replaced by the lifetime damage equivalent load for a specific turbine component.

Using Table 5.1 from the TotalControl Deliverable report D2.1, provides a scaling law for the determination of ε , as in:

TABLE 5.1: SCALING LAW FROM LOAD REDUCTION TO COMPONENT MASS REDUCTION

Component	Load ratio (α)	Strength	Fatigue	Deflection
<i>Blades</i>	<i>M-driven</i>	$\varepsilon = \alpha^{2/3}$		$\varepsilon = (\alpha/d)^{1/2}$
<i>Main Shaft</i>	<i>Torsion</i>		$\varepsilon = \alpha^{2/3}$	
<i>Tower, monopile</i>	<i>M-driven</i>		$\varepsilon = \alpha^{2/3}$	$\varepsilon = (\alpha/d)^{1/2}$

Assuming that the design in a component is dominated by one of the factors given in the above table, it implies that the mass of the component scales by a factor that can be computed based on the load change; for example, the mass of the support structure changes to the power (2/3) of the relative bending moment change. This would therefore imply a longer lifetime for the same design without de-rating and assuming the mass benefit can directly translate to cost benefit, the OPEX reduction would also follow the ε profiles shown in Table 5.1.

Since a load reduction would imply a lifetime increase for the same fatigue damage equivalent load target, the increase in lifetime can be converted to an increase in AEP to determine the reduction in LCOE. This is often a more robust estimate of the reduction in LCOE as compared to estimating

the reduction in OPEX, as the OPEX reduction also is dependent on the maintenance costs resulting from failures that are non-load dependent, which are not considered here. Therefore the LCOE quantification is made using the increase in life approach.

This lifetime increase from de-rating is sensitive to the magnitude of the exponent in the fatigue life curve (S-N curve) as well as by the duration of de-rating of the wind turbines. Assuming a de-rating by 20% over all mean wind speeds for 10% of the operational time for a single row of leading wind turbines was shown in chapter 3 to be able to be able to increase the lifetime by at least 5-10 years. Table 5.2 provides an estimate of the AEP increase and LCOE reduction assuming a 5 year increase in lifetime.

TABLE 5.2: LIFE INCREASE TO REDUCTION IN LCOE FOR THE LILLGRUND WIND FARM

	Increased life	Notes and assumptions
A. Increase in life	5 years	Based on de-rating the leading turbine row by 20% over all mean wind speeds for 10% of the operational time.
B. Increase in AEP from De-rating	2.0%	Estimation using results from previous sections without considering Life Extension
C. Increase in AEP with De-rating and life extension	4.0%	Combined benefit from A and B
D. Increase in lifetime costs	1.1%	Assume annual OPEX is €60/KWH
E. LCoE reduction	3.0%	Benefit from increase life production

While the values in Table 5.2 are an example, their overall magnitude is realistic. Increases in lifetime may be limited by other extraneous factors such as the electricity pricing structure, the maintenance contract upon life extension, the local regulations etc. The results presented in table 5.2 show that there is a large potential for LCOE reduction by using control strategies that reduce the loads and increase the lifetime of the components. The benefits accrue further with integration with wind farm ancillary services such as reactive power control.

6. CONCLUSIONS

The methodology implemented focused on utilizing artificial neural networks to predict mechanical loading and power production from wind turbines within a wind farm by training the networks using the results from aeroelastic load simulations. The results of the predictions were validated with load measurements on a single wind turbine in the farm as well as with power production from all wind turbines. The focus of the model and load simulations was the Lillgrund wind farm. The ANN was trained using full wind farm load simulations in the HAWC2 software that utilized the dynamic wake meandering model to quantify wake effects.

Selective de-rating of wind turbines was carried out and it was determined that de-rating the second row of wind turbines in the farm showed the best results in terms of increasing the net energy production and reducing the fatigue damage equivalent loads. A probabilistic assessment of variation in the fatigue damage to wind turbine structures in the farm was carried out to determine the reliability levels at different wind turbine positions, thereby allowing for potential balanced fatigue lifetime consumption throughout the farm using farm control without sacrificing the desired power production level. This allowed computationally fast quantification of reliability levels of turbine components which can be used to assess the reliability against the target design level.

The results showed significant operational gains: the power lost due to de-rating the second row was more than compensated by power gains deeper in the wind farm, where some of the most highly loaded turbines had increased power productions of upto 40% at lower wind speeds. The net AEP increase of the wind farm with de-rating was about 2% and with an estimated 5 years increase in lifetime, a net AEP increase of 4% was quantified, which resulted in an LCOE reduction of 3%.

REFERENCES

- [1]. IEC, "International Electro technical Committee, IEC 61400-1: Wind Turbines Part- 1: Design Requirements." Edition 4, Geneva, 2019.
- [2] Jackson G Njiri, Yan Liu, and Dirk Söffker. "Multivariable control of large variable-speed wind turbines for generator power regulation and load reduction". In: IFAC-PapersOnLine 48.1 (2015), pp. 544–549.
- [3] Torben Knudsen, Thomas Bak, and Mikael Svenstrup. "Survey of wind farm control—power and fatigue optimization". In: Wind Energy 18.8 (2015), pp. 1333–1351.
- [4] Daria Madjidian, Karl Martensson, and Anders Rantzer. "A distributed power coordination scheme for fatigue load reduction in wind farms". In: Proceedings of the 2011 American Control Conference (2011), pp. 5219–5224.
- [5] Stefanos Baros and Anuradha M Annaswamy. "Distributed optimal wind farm control for fatigue load minimization: A consensus approach". In: International Journal of Electrical Power & Energy Systems 112 (2019), pp. 452–459.
- [6] Jackson G Njiri et al. "Consideration of lifetime and fatigue load in wind turbine control". In: Renewable energy 131 (2019), pp. 818–828.
- [7] Anand Natarajan, Troels F Pedersen, et al. "Remaining Life Assessment of Offshore Wind Turbines subject to Curtailment". In: The 28th International Ocean and Polar Engineering Conference .International Society of Offshore and Polar Engineers. 2018.
- [8] Natarajan, A. "An overview of the state of the art technologies for multi-MW scale offshore wind turbines and beyond". Wiley Interdisciplinary Reviews: Energy and Environment, Vol. 3, No. 2, 2014, pp. 111-121.
- [9] James Lindsay et al. Wind turbine reliability: a database and analysis approach. Tech. rep. Sandia National Laboratories, 2008.
- [10] W Hwang and KS Han. "Cumulative damage models and multi-stress fatigue life prediction". In: Journal of composite materials 20.2 (1986), pp. 125–153.
- [11] Dimitrov, N. K. Surrogate models for parameterized representation of wake-induced loads in wind farms. *Wind Energy*, 22(10), 2019, 1371–1389.
- [12] Dimitrov, N. K., & Natarajan, A. From SCADA to lifetime assessment and performance optimization: how to use models and machine learning to extract useful insights from limited data. *Journal of Physics: Conference Series (Online)*, 1222(Conf. 1), 2019
- [13] Larsen, T.J, Hansen, A.M. (2015). "How 2 HAWC2, the user's manual". Dept. of Wind Energy Report no. DTU Risoe-R-1597. Technical University of Denmark
- [14] Fleming, P. et. al. (2017). Field test of wake steering at an offshore wind farm, *Wind Energy Science Journal*, 2, 229–239.
- [15] Dimitrov, N. K., Kelly, M. C., Vignaroli, A., & Berg, J. (2018). From wind to loads: wind turbine site-specific load estimation with surrogate models trained on high-fidelity load databases. *Wind Energy Science*, 3(2), 767-790.
- [16] Larsen G. C., Madsen H. A., Thomsen, K. and Larsen T. J. (2008). Wake meandering – a pragmatic approach. *Wind Energy* 11, pp. 377–395.
- [17] Galinos C., Dimitrov N., Larsen T. J., Natarajan A., Hansen K. S.(2016) Mapping Wind Farm Loads and Power Production - A Case Study on Horns Rev 1. *Journal of Physics: Conference Series* 753(3), article number 032010